

ANCHORING ENTITIES: RETRIEVAL-AUGMENTED HALLUCINATION DETECTION

000
001
002
003
004
005 **Anonymous authors**
006 Paper under double-blind review
007
008
009
010

ABSTRACT

011 Hallucination detection is crucial for large language models (LLMs), as hallu-
012 cinated content creates significant barriers in applications requiring factual accu-
013 racy. Current detection methods mainly depend on internal signals like uncertainty
014 and self-consistency checks, using the model’s pre-trained knowledge to identify
015 unreliable outputs. However, pre-trained knowledge may become outdated and
016 has coverage limitations, especially for specialized or recent information. To ad-
017 dress these limitations, retrieval-augmented generation (RAG) has emerged as a
018 promising solution that grounds model outputs in external evidence. In this pa-
019 per, we target a critical and practical learning problem *RAG-based hallucination*
020 *detection* (RHD), where RAG is employed to enhance hallucination detection by
021 addressing information updating challenges. To address RHD, we propose a novel
022 method *Evidence-Aligned Entity Verification* (EAEV), which detects entity-level
023 hallucinations by leveraging RAG to align generated entities with retrieved evi-
024 dence contexts. Specifically, EAEV evaluates entity-evidence alignment through
025 three complementary dimensions and introduces counterfactual stability analysis
026 to ensure robust alignments under evidence perturbations. Experiments across
027 multiple RAG benchmarks demonstrate that EAEV achieves consistent improve-
028 ments over existing methods with strong generalization capabilities.
029

1 INTRODUCTION

030 The deployment of large language models (LLMs) in practical applications faces a critical challenge:
031 models frequently generate factually incorrect or inconsistent content, known as hallucinations (Ji
032 et al., 2023). This problem poses significant risks in domains where accuracy is essential, such as
033 medical diagnosis, educational assistance, and financial advisory services (Tang et al., 2024; Wang
034 et al., 2024). As organizations increasingly rely on LLMs for complex tasks, the consequences of
035 undetected hallucinations can range from misinformation propagation to decision-making failures,
036 making robust hallucination detection an urgent priority for trustworthy AI deployment.
037

038 Existing hallucination detection methods have established foundations across diverse paradigms.
039 Uncertainty-based approaches leverage model confidence signals and entropy to identify potentially
040 unreliable outputs (Manakul et al., 2023; Farquhar et al., 2024). Consistency-based methods eval-
041 uate factual reliability through cross-generation agreement and semantic coherence (Li et al., 2023).
042 More recently, attention-based interpretability techniques and representational analysis have pro-
043 vided mechanistic insights into when models exhibit knowledge awareness versus hallucination
044 tendencies (Azaria & Mitchell, 2023; Burns et al., 2022). These methods perform well in their
045 evaluation settings and rely primarily on internal model signals for detection decisions.

046 However, traditional detection approaches face fundamental limitations when deployed in real-world
047 applications. As illustrated in Figure 1, models often generate hallucinations about recent events,
048 specialized domains, or rapidly evolving information that falls outside their training data coverage
049 (Mallen et al., 2022). Additionally, reliance on internal model signals makes these methods vuln-
050 erable to distribution shifts and domain-specific biases that can compromise detection reliability. To
051 address these coverage and recency limitations, retrieval-augmented generation (RAG) has emerged
052 as a promising solution that grounds model outputs in external evidence sources (Lewis et al., 2020;
053 Gao et al., 2023). RAG systems dynamically incorporate relevant documents during generation, en-
abling models to access up-to-date information while providing explicit evidence for factual claims.

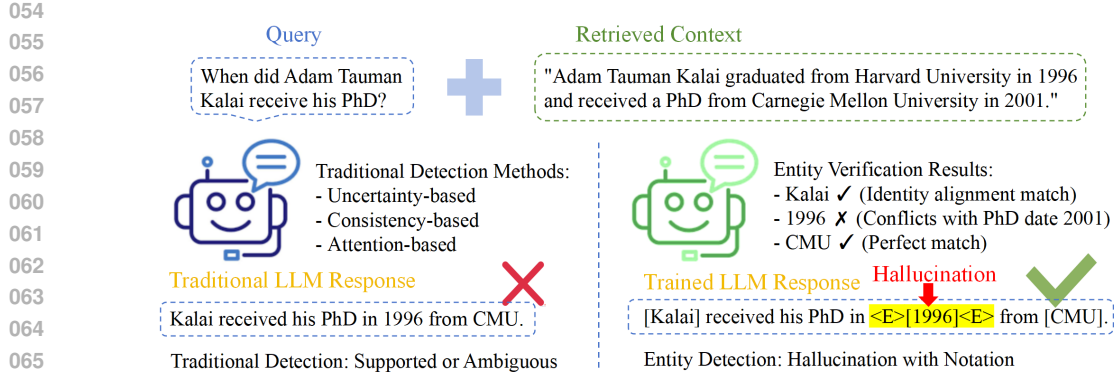


Figure 1: Comparison of traditional and RAG-based entity hallucination detection methods.
Example adapted from (OpenAI, 2025).

Despite the promise of evidence-grounded generation, RAG introduces distinct challenges that expose new hallucination detection requirements. Models frequently fabricate entities even when correct information exists within context window, creating misalignments between retrieved evidence and generated content (Niu et al., 2024). Current detection methods typically rely on external judge models for verification, which introduce additional complexity and potential error propagation while operating at token, sentence, or paragraph levels that miss the entity-level factual commitments users most critically evaluate (Yue et al., 2023). This disconnect between detection granularity and user verification behavior motivates a specialized approach to evidence-based hallucination detection.

Addressing these challenges requires overcoming fundamental obstacles that distinguish RAG-based detection from traditional approaches. The spurious correlation problem occurs when hallucinated entities accidentally align with retrieved text through surface-level keyword matches, creating false signals of evidence support. The need for precise localization of factual inconsistencies at the entity level becomes critical, as entities constitute the atomic units of factual information that users prioritize when evaluating response trustworthiness (Thorne et al., 2018). When critical entities such as names, dates, or quantities contain errors, user confidence in the entire response deteriorates regardless of overall semantic coherence. This motivates our central question:

How can we leverage RAG to enhance hallucination detection by establishing direct entity-evidence alignment within retrieved contexts?

Building on this foundation, we propose Evidence-Aligned Entity Verification (EAEV), a novel method that operates entirely within retrieved contexts to verify entity mentions through complementary alignment mechanisms. EAEV evaluates each entity along three dimensions: identity alignment for direct matches, semantic alignment for paraphrases, and consistency alignment for quantitative attributes and conflicts. To address spurious correlations, EAEV incorporates counterfactual stability analysis that distinguishes robust evidence support from fragile alignments. Extensive experiments demonstrate EAEV’s effectiveness, achieving 87.89% AUROC on LLaMA2-13B with strong generalization across datasets. Our main contributions are summarized as follows:

- We establish *RAG-based hallucination detection* (RHD) as a novel problem formulation that leverages RAG for entity-level verification within retrieved contexts, tackling the remaining challenge that prior methods rely on internal uncertainty or external judges without evidence traceability.
- We propose *Evidence-Aligned Entity Verification* (EAEV), a novel method that combines multi-dimensional alignment with counterfactual stability analysis to distinguish genuine evidence support from spurious correlations in RAG settings.
- We demonstrate superior performance and generalization across multiple RAG benchmarks and model architectures, achieving state-of-the-art results while maintaining practical deployability.

2 PRELIMINARY

In this section, we present necessary notations and establish the theoretical foundation for RAG-based hallucination detection, emphasizing entity-centric verification within retrieved contexts.

108 **Basic Definitions** Following standard conventions, we represent an LLM as a probability dis-
 109 tribution $P_\theta(\cdot)$ over token sequences, where θ denotes the model parameters. Given a query
 110 $q = [x_1, \dots, x_k]$, the model generates an answer $Y = [x_{k+1}, \dots, x_{k+l}]$ through autoregressive
 111 prediction $P_\theta(x_j|x_1, \dots, x_{j-1})$. For dataset representation, each instance consists of a query q ,
 112 generated answer Y , and retrieved context passages $\mathcal{P} = \{p_k\}_{k=1}^K$. Each answer receives a binary
 113 hallucination label $y \in \{0, 1\}$ where $y = 1$ indicates truthful content.

114
 115 **Traditional Hallucination Detection** Traditional hallucination detection aims to identify factu-
 116 ally incorrect content in LLM outputs. Given a query q and answer Y , a detector D produces
 117 $\hat{y} = D(q, Y)$ where $\hat{y} \in \{0, 1\}$ indicates hallucination presence. Existing methods operate through
 118 uncertainty estimation, consistency checking, or external verification, but face challenges when evi-
 119 dence is explicitly available yet underutilized in RAG settings.

120
 121 **RAG-based Hallucination Detection** RAG-based hallucination detection (RHD) represents a
 122 fundamental shift from traditional approaches by leveraging retrieved evidence for verification. Un-
 123 like conventional methods that rely solely on model internals, RHD operates under the assumption
 124 that factual accuracy can be determined through explicit alignment between generated content and
 125 available evidence within retrieved contexts \mathcal{P} . We formalize RHD as follows:

126 Given a query q , retrieved contexts \mathcal{P} , and generated answer Y , the objective of RHD is to learn a
 127 detector D that determines factual accuracy through evidence alignment:

$$128 \quad D(q, Y, \mathcal{P}) = \begin{cases} 1, & \text{if } Y \text{ is supported by evidence in } \mathcal{P}, \\ 129 \quad 0, & \text{otherwise.} \end{cases} \quad (1)$$

131 The key insight is that factual errors in RAG settings manifest primarily at the entity level, where
 132 specific named entities, temporal expressions, and quantities determine overall response reliability.

133
 134 **Entity-Centric Verification Framework** For entity-centric verification, we extract candidate
 135 mentions s from the generated answer Y , where each mention has type $t \in \{\text{ENT}, \text{NUM}, \text{NP}\}$ cor-
 136 responding to named entities, numerical values, and noun phrases. For each mention s , we retrieve
 137 evidence windows from \mathcal{P} and select primary evidence e^* through relevance scoring. We define
 138 three core alignment functions: identity alignment $\text{Id}(s, e^*) \in [0, 1]$ measuring surface correspon-
 139 dence, semantic alignment $\text{Sem}(s, e^*) \in [-1, 1]$ capturing meaning preservation, and consistency
 140 alignment $\text{Con}(s, e^*) \in [0, 1]$ evaluating quantitative agreement and conflict detection.

141 For each mention s , we compute support signals through weighted combination of alignment dimen-
 142 sions and detect conflicts through binary indicators. To distinguish robust evidence from spurious
 143 correlations, we apply counterfactual stability analysis using perturbation sets \mathcal{U} . Finally, mentions
 144 are aggregated into entity-level decisions through canonicalization, producing interpretable verifi-
 145 cation scores with direct evidence traceability.

146

147 3 METHODOLOGY

148

149 3.1 MOTIVATION AND OBSERVATIONS

150

151 Effective RAG verification requires understanding how factual errors manifest in the presence of
 152 relevant evidence. As illustrated in Figure 1, traditional hallucination detection methods rely solely
 153 on internal model signals and are limited by training data coverage, while our RAG-enhanced
 154 approach incorporates external evidence sources to improve detection accuracy and coverage. Con-
 155 sider a model given documents stating “Adam Tauman Kalai graduated from Harvard University in
 156 1996 and received a PhD from Carnegie Mellon University in 2001” but generating “Kalai received
 157 his PhD in 1996 from CMU” (OpenAI, 2025). This example illustrates a fundamental challenge:
 158 models can fabricate specific entities while correctly incorporating other factual elements from the
 159 context, as noted by recent analysis of why language models hallucinate.

160

161

162 Existing detection methods operating at sentence or paragraph levels fail to localize such precise fac-
 163 tual inconsistencies, as the overall semantic coherence remains high despite the critical entity-level
 164 error. Empirical analysis across RAG benchmarks reveals that entity-level inconsistencies constitute

162 the primary failure mode, with named entities, dates, and quantities representing the most frequent
 163 error types that directly impact user trust and system reliability. This observation motivates our
 164 entity-centric approach: rather than evaluating global semantic consistency, we decompose verifica-
 165 tion into atomic factual units where evidence alignment can be precisely established and traced.
 166

167 3.2 FRAMEWORK OVERVIEW

169 To address these challenges, we propose EAEV, which transforms entity verification into a system-
 170 atic evidence alignment task through four interconnected stages that maintain evidence traceability
 171 throughout verification. As shown in Figure 2, the framework operates under three core principles:
 172 context-only verification where all signals derive from alignment between generated content and
 173 retrieved evidence, entity-centric aggregation enabling cross-mention evidence consolidation, and
 174 unified verification architecture supporting both rule-based decisions and model fine-tuning.

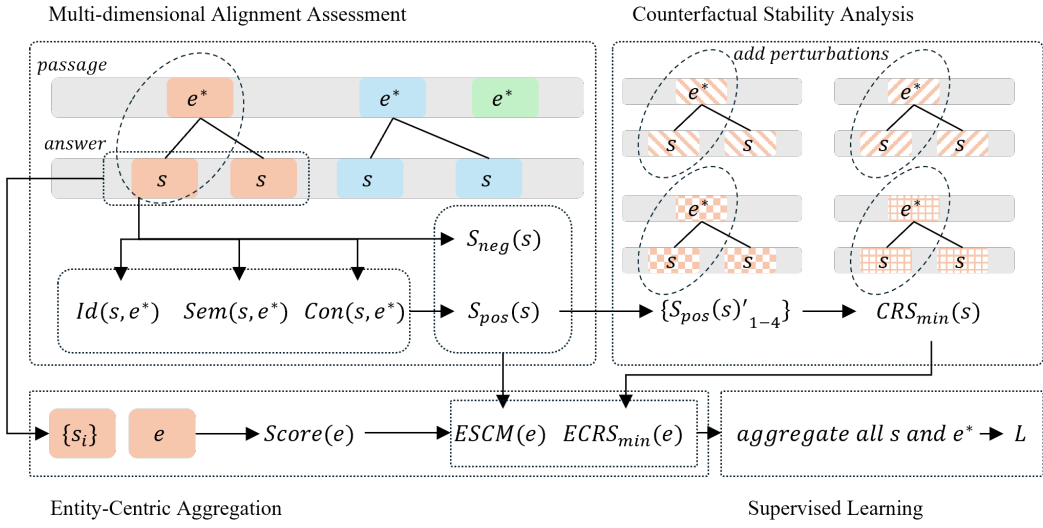


Figure 2: Framework Overview of our Methodology.

194 Given a query q , retrieved context \mathcal{P} , and generated answer Y , EAEV proceeds through: (1) *candidate*
 195 *mention extraction* that identifies factual commitments in Y and constructs local answer windows,
 196 (2) *evidence retrieval and selection* that retrieves top-k evidence windows from \mathcal{P} and selects
 197 primary evidence e^* by maximizing relevance scores combining identity and semantic similarity,
 198 (3) *multi-dimensional alignment assessment* that evaluates entity-evidence correspondence through
 199 complementary signals while testing robustness via stability analysis, and (4) *entity-centric aggregation*
 200 that consolidates mention-level signals into entity-level decisions and produces span, entity,
 201 and answer-level verification outputs. This modular design enables comprehensive verification while
 202 preserving evidence traceability for interpretable decisions.

203 3.3 MULTI-DIMENSIONAL ALIGNMENT ASSESSMENT

205 For each candidate mention s extracted from the answer and its selected primary evidence e^* from
 206 the retrieved context, we evaluate alignment through three complementary dimensions that capture
 207 orthogonal aspects of evidential support.

209 **Identity Alignment** Identity alignment captures direct matches through lexical forms and aliases,
 210 providing precise signals for exact alignment. This dimension uses a normalized similarity function
 211 that blends exact substring matching with fuzzy token-level matching:

$$Id(s, e^*) = \max(\mathbb{I}[s \subseteq e^* \vee e^* \subseteq s], TSR(s, e^*)) \quad (2)$$

213 where $\mathbb{I}[\cdot]$ is the indicator function and $TSR(s, e^*) \in [0, 1]$ computes the normalized token set ratio
 214 measuring lexical overlap between mention and evidence tokens. This formulation prioritizes exact
 215 matches while gracefully handling orthographic variations and aliases through the fuzzy matching
 fallback, ensuring robust identity detection across diverse lexical forms.

216 **Semantic Alignment** Semantic alignment evaluates meaning preservation through embedding
 217 similarity, capturing paraphrases and reformulations that maintain factual content despite variations:
 218

$$\text{Sem}(s, e^*) = \cos(f_{\text{enc}}(s), f_{\text{enc}}(e^*)) \quad (3)$$

220 where $f_{\text{enc}}(\cdot)$ represents sentence-level embedding encoding that captures semantic correspondence
 221 beyond explicit textual correspondence. This approach enables detection of semantically equivalent
 222 expressions while maintaining computational efficiency, though it requires careful calibration to
 223 prevent accepting spurious semantic matches that lack genuine factual grounding.

224 **Consistency Alignment** Consistency alignment addresses value correspondence and explicit factual
 225 conflicts through numerical overlap assessment combined with rule-based contradiction detection.
 226 For entities with quantitative attributes, we measure consistency through normalized intersection
 227 over union of extracted numerical values:
 228

$$\text{Con}(s, e^*) = \frac{|N(s) \cap N(e^*)|}{|N(s) \cup N(e^*)|} + b_{\text{anc}} \cdot \mathbb{I}[\text{anchor}(q, e^*)] \quad (4)$$

231 where $N(\cdot)$ extracts and normalizes numerical values from text, and b_{anc} provides an anchor bonus
 232 when evidence contains key terms from the original query, strengthening confidence in relevant retrievals.
 233 Additionally, we detect explicit contradictions through $S_{\text{neg}}(s) \in \{0, 1\}$ using rule-based
 234 patterns that identify temporal mismatches, numerical conflicts, and relational inconsistencies, pro-
 235 viding high-precision negative signals that complement the positive consistency scores.

236 **Type-Adaptive Support Synthesis** We synthesize the three alignment dimensions into a unified
 237 support score that adapts to mention types, recognizing that different entity categories require different
 238 verification emphases. For each mention s of type $t \in \{\text{ENT, NUM, NP}\}$, we compute positive
 239 support signals $S_{\text{pos}}(s) \in [0, 1]$ through weighted combination of alignment dimensions:
 240

$$S_{\text{pos}}(s) = w_I^{(t)} \cdot \text{Id}(s, e^*) + w_S^{(t)} \cdot \text{Sem}(s, e^*) + w_C^{(t)} \cdot \text{Con}(s, e^*) \quad (5)$$

243 where type-adaptive weights $w_I^{(t)}, w_S^{(t)}, w_C^{(t)}$ are optimized for each mention type—numerical men-
 244 tions emphasize consistency alignment while named entities prioritize identity and semantic align-
 245 ment. Additionally, we detect explicit conflicts through binary indicators $S_{\text{neg}}(s) \in \{0, 1\}$ using rule-based
 246 patterns that identify temporal mismatches, numerical conflicts, and relational inconsis-
 247 tencies. We then compute a consistency margin $\text{SCM}(s) = S_{\text{pos}}(s) - \beta \cdot S_{\text{neg}}(s)$ where β controls
 248 conflict penalties, integrating positive evidence support with negative conflict signals.

249 3.4 COUNTERFACTUAL STABILITY ANALYSIS

251 A critical challenge in RAG-based verification is distinguishing genuine evidence support from spu-
 252 rious correlations, where hallucinated content accidentally matches retrieved text through surface-
 253 level similarities. Traditional alignment metrics can be deceived by coincidental keyword overlaps
 254 or formatting artifacts that create false signals of factual support. To address this fundamental prob-
 255 lem, we propose counterfactual stability analysis that tests whether evidence alignment remains
 256 robust under controlled perturbations.

257 The core insight is that genuine factual correspondence should persist across minor variations in
 258 text presentation, while spurious matches are inherently fragile and collapse when surface features
 259 change. We define perturbation sets \mathcal{U} containing controlled variations that preserve semantic con-
 260 tent while altering surface characteristics. For each mention s , we compute stability bounds: mini-
 261 mum support $\text{CRS}_{\min}(s) = \min_{u \in \mathcal{U}} S_{\text{pos}}^{(u)}(s)$ measuring the lowest support under perturbations, and
 262 stability gaps $\text{CRS}_{\Delta}(s) = S_{\text{pos}}(s) - \text{CRS}_{\min}(s)$ indicating robustness to variations.

263 We instantiate \mathcal{U} with four targeted perturbations that address distinct sources of spurious corre-
 264 lation: (1) *leave-one-out evidence removal* eliminates the strongest evidence window to test depen-
 265 dency on single sources, preventing over-reliance on potentially misleading context; (2) *punctuation*
 266 and *case normalization* removes formatting artifacts and capitalization patterns creating false lex-
 267 ical matches, ensuring alignment reflects genuine content rather than presentation; (3) *whitespace*
 268 *compression* eliminates spacing variations and tokenization inconsistencies that might artificially
 269 inflate similarity scores; and (4) *alphanumeric-only filtering* retains only core semantic content by
 removing symbols and special characters that could create spurious token-level alignments.

270 High minimum support $CRS_{\min}(s)$ indicates that evidence alignment persists across these controlled
 271 variations, indicating the factual correspondence is robust rather than circumstantial. Conversely,
 272 large stability gaps $CRS_{\Delta}(s)$ reveal fragile correlations that depend on specific textual configura-
 273 tions, flagging potentially unreliable evidence support. This stability analysis enables EAEV to dis-
 274tinguish authentic factual grounding from accidental surface-level matches, significantly improving
 275 detection precision in challenging cases where traditional alignment metrics alone prove insufficient.
 276

277 3.5 ENTITY-CENTRIC AGGREGATION

279 For entities with multiple mentions across the answer, we consolidate evidence signals to obtain
 280 robust entity-level assessments. We canonicalize mention strings through lowercasing, punctuation
 281 and article removal to identify coreferent mentions, and apply lightweight pronoun resolution that
 282 links pronouns to the most recent non-pronoun entity.

283 For an entity e with mention set $\{s_i\}$, we aggregate verification signals conservatively. Positive
 284 support uses top-K averaging $ES_{\text{pos}}(e) = \text{mean}(\text{topK}\{S_{\text{pos}}(s_i)\})$ to emphasize strongest evidence
 285 across mentions. Negative signals use max pooling $ES_{\text{neg}}(e) = \max\{S_{\text{neg}}(s_i)\}$ for conservative
 286 conflict detection, ensuring any mention-level conflict propagates to entity level. Stability becomes
 287 $ECRS_{\min}(e) = \min\{CRS_{\min}(s_i)\}$ to identify the weakest link across all entity mentions.

288 The entity consistency margin $ESCM(e) = ES_{\text{pos}}(e) - \beta_e \cdot ES_{\text{neg}}(e)$ integrates these consolidated
 289 signals, where β_e controls entity-level conflict penalties. The final entity verification score integrates
 290 consistency and stability through a multiplicative combination:

$$291 \text{score}(e) = \sigma(-ESCM(e)) \cdot (1 - \sigma(ECRS_{\min}(e))) \quad (6)$$

293 where $\sigma(\cdot)$ denotes the sigmoid function. This formulation produces high risk scores for entities
 294 with weak evidence support or low stability, enabling answer-level assessment through max pooling
 295 over entity scores while preserving traceability to specific evidence windows.

296 3.6 EAEV-GUIDED SUPERVISED LEARNING

298 The alignment and stability signals computed by EAEV provide direct supervision for training mod-
 299els to perform interpretable hallucination detection through entity-level annotation. Rather than
 300 requiring complex architectural modifications, we leverage EAEV’s verification capabilities to con-
 301struct high-quality training data where models learn to reproduce answers while marking unsup-
 302 ported entities with verification tags.

303 For each training instance, we generate target sequences where entities with $ESCM(e) < \tau_{\text{threshold}}$
 304 are enclosed in $\langle E \rangle$ markers, creating supervision that directly transfers EAEV’s multi-dimensional
 305 verification logic to generation. We optimize a token-weighted cross-entropy that transfers EAEV’s
 306 entity-level signals into generation:

$$308 L = \sum_t w_t \cdot \text{CE}(p_{\theta}(y_t | x, y_{<t}), y_t) \quad (7)$$

310 where

$$312 w_t = \text{clip} \left(1 + \alpha \cdot \max_{e \ni t} \sigma(-ESCM(e)) + \gamma \cdot \max_{e \ni t} (1 - \sigma(ECRS_{\min}(e))), w_{\min}, w_{\max} \right) \quad (8)$$

314 and tokens outside any tagged entity use $\max_{e \ni t} = 0$. This approach enables standard supervised
 315 fine-tuning to learn EAEV’s sophisticated verification patterns, transferring interpretable entity-level
 316 detection capabilities into generation without requiring specialized decoding procedures or multi-
 317 model coordination.

318

319 4 EXPERIMENT

320

321 4.1 EXPERIMENT SETTINGS

322

Datasets We evaluate EAEV across three representative RAG hallucination benchmarks that cover
 323 diverse reasoning scenarios and evaluation granularities. **RAGTruth** provides high-quality manual

324 annotations with nearly 18,000 responses from multiple LLMs across question answering, data-to-
 325 text generation, and news summarization tasks, offering fine-grained word-level annotations that
 326 we aggregate to answer-level evaluation (Niu et al., 2024). **HotpotQA** represents multi-hop rea-
 327 soning challenges built on Wikipedia articles with sentence-level supporting facts, requiring cross-
 328 document evidence synthesis for accurate verification (Yang et al., 2018). **DelucionQA** focuses
 329 on domain-specific hallucinations in automotive manuals with human-annotated labels, providing
 330 specialized evaluation for technical content verification (Sadat et al., 2023). More details of the
 331 datasets could be found in Appendix. This dataset combination ensures comprehensive evaluation
 332 across commonsense reasoning, knowledge-intensive tasks, and domain-specific applications while
 333 maintaining consistency in answer-level hallucination assessment.

334
 335 **Baselines** We conduct experiments on three representative LLMs: Qwen2.5-7B (Yang et al.,
 336 2024), LLaMA2-7B (Touvron et al., 2023), and LLaMA2-13B (Touvron et al., 2023). For hallu-
 337 cination detection methods, we compare against eleven state-of-the-art baselines spanning different
 338 detection paradigms. Uncertainty-based approaches include **SelfCheckGPT** (Manakul et al., 2023),
 339 **Semantic Entropy** (Kuhn et al., 2023), and **LLM-Check** (Jain et al., 2024), which leverage model
 340 confidence signals and internal activations for detection. Consistency-based methods such as **Early-**
 341 **Detect** (Snyder et al., 2024) and **NoVo** (Ho et al., 2024) evaluate reliability through cross-generation
 342 agreement and attention-level analysis. RAG-specific approaches include **RAGAS** (Es et al., 2024),
 343 **RefChecker** (Hu et al., 2024), **ReDEeP** (Sun et al., 2024), and **TSV** (Park et al., 2025), which ex-
 344 plicitly incorporate retrieved evidence for verification. We also include general detection methods
 345 **Linear Probe** (Duan et al., 2024) and **HaloScope** (Du et al., 2024) that operate on model represen-
 346 tations. We evaluate all methods using AUROC, Accuracy, and F1 score as our primary metrics to
 347 ensure comprehensive performance assessment. Detailed baseline configurations and implemen-
 348 tation details are provided in the Appendix B and A.1.2.

349 4.2 EXPERIMENTAL RESULTS AND ANALYSIS

350
 351 **Main Results** EAEV achieves consistent superiority across all evaluation settings, demonstrating
 352 the effectiveness of entity-centric evidence alignment for RAG hallucination detection. As shown in
 353 Table 1, our method attains 85.93% average AUROC on Qwen2.5-7B, 84.25% on LLaMA2-7B, and
 354 87.55% on LLaMA2-13B, representing substantial improvements of 2.80, 2.40, and 3.34 percentage
 355 points respectively over the strongest baseline TSV. The robustness of performance across diverse
 356 model architectures validates our core hypothesis that entity-level factual errors constitute a model-
 357 agnostic challenge in RAG systems. Notably, larger models show particularly pronounced improve-
 358 ments, with LLaMA2-13B achieving the highest absolute performance, suggesting that EAEV ef-
 359 fectively leverages enhanced model capabilities for more sophisticated evidence alignment while
 360 maintaining consistent gains across different architectural families.

361
 362 Cross-dataset evaluation reveals EAEV’s strong generalization capabilities across diverse reasoning
 363 scenarios and domain requirements. On RAGTruth’s fine-grained annotations, our method achieves
 364 the most substantial improvements, demonstrating effectiveness in detecting nuanced factual incon-
 365 sistencies within general knowledge contexts. HotpotQA results highlight EAEV’s strength in multi-
 366 hop reasoning scenarios, where our consistency alignment mechanism proves particularly valuable
 367 for verifying complex logical chains that span multiple evidence sources. DelucionQA performance
 368 validates applicability to specialized technical domains, where entity verification demands precision
 369 in handling domain-specific terminology and quantitative relationships. This consistent performance
 370 across datasets with fundamentally different characteristics—from general knowledge to multi-hop
 371 reasoning to technical domains—confirms that our multi-dimensional alignment framework captures
 372 universal patterns in entity-level hallucination detection rather than dataset-specific artifacts.

373
 374 The performance scaling pattern provides additional validation of our design principles while high-
 375 lighting EAEV’s practical deployability across diverse computational environments. Both 7B and
 376 13B model variants benefit significantly from our approach, with the scaling behavior indicating
 377 that our framework harnesses enhanced model capabilities without sacrificing robustness at smaller
 378 scales. This versatility enables deployment in resource-constrained settings requiring smaller mod-
 379 els while maximizing performance in high-capacity applications. The consistent benefits across all
 380 tested architectures, combined with our method’s ability to achieve state-of-the-art results through

378 Table 1: Performance comparison across different models and datasets. We report AUROC, Acc-
 379 racy (Acc), and F1 scores for each method on three datasets. All results are averaged over three
 380 independent runs, with the rightmost columns showing metrics averaged across datasets.

Method	RAGTruth			HotpotQA			DelucionQA			Average		
	AUROC	Acc	F1	AUROC	Acc	F1	AUROC	Acc	F1	AUROC	Avg Acc	Avg F1
<i>Qwen2.5-7B</i>												
EarlyDetect	66.38	70.12	65.34	67.15	69.32	65.10	68.25	69.83	66.21	67.24	69.72	65.55
Selfcheckgpt	64.39	69.05	63.28	65.73	68.32	63.95	66.43	68.76	65.01	65.51	68.71	64.08
Novo	73.79	76.21	68.67	74.85	75.75	69.12	76.03	76.12	70.43	74.89	76.01	69.44
Linear Probe	75.27	77.38	69.52	76.11	77.02	69.84	77.10	77.54	71.02	76.16	77.31	70.13
HaloScope	71.01	74.16	67.70	72.24	73.90	68.20	73.01	74.16	69.05	72.08	74.05	68.32
LLM-Check	62.75	68.07	62.18	63.91	67.20	62.93	65.14	67.86	64.23	63.93	67.71	63.09
Semantic Entropy	65.43	70.65	64.71	66.87	69.83	65.25	68.02	70.19	65.84	66.75	70.19	65.27
RAGAS	74.76	77.32	69.90	76.02	76.84	70.40	76.89	77.01	71.43	75.89	77.06	70.58
RefCheck	73.25	75.89	68.43	74.61	75.30	68.81	75.20	75.76	70.01	74.35	75.65	69.08
ReDEeP	77.87	78.51	71.92	79.43	78.23	72.74	80.12	78.96	73.52	79.14	78.57	72.71
TSV	81.45	79.83	72.37	82.07	79.36	72.28	85.87	80.47	74.97	83.13	79.89	73.21
EAEV (Ours)	85.36	80.04	74.28	86.74	81.23	74.35	85.68	80.25	75.62	85.93	80.51	74.75
<i>LLaMA2-7B</i>												
EarlyDetect	65.12	68.87	63.98	66.23	68.05	63.55	67.12	68.42	64.33	66.16	68.42	63.95
Selfcheckgpt	63.18	67.31	62.01	64.45	66.25	62.74	65.37	66.90	63.45	64.33	66.82	62.72
Novo	72.25	75.28	67.12	73.31	74.82	67.62	74.38	75.01	68.92	73.31	75.03	67.89
Linear Probe	73.56	76.36	68.23	74.25	75.43	68.55	75.48	75.62	70.02	74.44	75.68	68.92
HaloScope	69.83	73.24	66.31	70.92	72.43	66.75	71.74	73.25	67.45	70.83	72.96	66.82
LLM-Check	61.47	66.42	60.08	62.63	65.32	61.32	63.71	66.19	62.03	62.59	65.95	61.34
Semantic Entropy	64.12	69.01	63.43	65.25	68.32	63.78	66.30	69.02	64.01	65.22	68.78	63.71
RAGAS	73.11	76.25	68.11	74.43	75.62	68.75	75.45	76.12	70.12	74.33	76.69	68.99
RefCheck	71.66	74.83	66.92	73.08	74.41	67.30	74.02	74.88	68.15	72.92	74.71	67.46
ReDEeP	76.42	78.01	71.23	77.63	77.15	71.94	78.35	77.66	72.43	77.47	77.61	71.86
TSV	82.04	79.12	72.01	82.64	78.83	72.10	80.88	77.52	73.95	81.85	78.49	72.77
EAEV (Ours)	84.57	80.12	74.07	84.96	82.55	73.39	83.21	78.32	74.45	84.25	80.33	73.97
<i>LLaMA2-13B</i>												
EarlyDetect	67.18	70.01	65.12	68.42	69.05	65.87	69.66	69.81	66.50	68.42	69.62	65.83
Selfcheckgpt	65.47	68.10	63.02	66.93	67.22	63.89	67.82	67.88	64.52	66.74	67.73	63.81
Novo	74.81	76.35	69.31	75.84	76.11	70.16	77.12	76.55	71.22	75.92	76.34	70.21
Linear Probe	76.31	77.65	70.54	77.54	77.33	71.39	78.82	77.97	72.82	77.55	77.63	71.53
HaloScope	71.74	74.45	68.20	72.81	73.25	68.91	73.93	74.15	69.85	72.83	73.93	68.99
LLM-Check	63.83	67.12	61.95	65.28	66.52	62.73	66.55	66.98	63.45	65.19	66.87	62.71
Semantic Entropy	66.02	70.20	64.62	67.35	69.02	65.21	68.40	70.10	65.83	67.26	69.77	65.22
RAGAS	75.67	77.32	70.22	76.88	77.01	71.01	78.02	77.66	72.52	76.86	77.33	71.25
RefCheck	74.25	76.00	68.85	75.66	75.43	69.33	76.92	76.41	70.44	75.61	75.95	69.54
ReDEeP	78.93	79.63	72.33	80.11	79.25	73.21	81.04	79.81	74.15	80.03	79.56	73.23
TSV	84.55	80.12	73.50	83.12	79.43	73.22	84.96	80.12	75.68	84.21	79.89	74.13
EAEV (Ours)	87.89	84.29	76.85	88.12	83.53	75.59	86.65	83.22	77.92	87.55	83.68	76.79

413 entity-centric verification within retrieved contexts, establishes EAEV as a reliable and scalable
 414 solution for RAG hallucination detection across varied deployment scenarios.

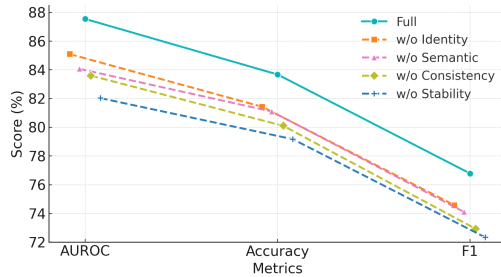
415
 416 **Ablation Study** To validate each component’s contribution, we conduct comprehensive ablation
 417 studies across all benchmarks. As shown in Figure 3a and Table 2, counterfactual stability analysis
 418 provides the most substantial contribution, confirming the necessity of our approach for distinguishing
 419 genuine evidence support from spurious correlations. The results demonstrate that each alignment
 420 dimension contributes meaningfully to overall performance, with balanced degradation patterns
 421 indicating that all components address distinct verification challenges. The full framework’s
 422 superior performance validates our multi-dimensional design philosophy and demonstrates syner-
 423 gistic effects among complementary alignment mechanisms. Details are provided in Appendix C.1.

424
 425 **Sensitivity Analysis** We analyze EAEV’s robustness to answer-side window length, a key pa-
 426 rameter controlling contextual span during evidence alignment. As shown in Figure 3b, the frame-
 427 work achieves optimal performance with 30-token windows while maintaining stability across the
 428 practical range. Smaller windows limit contextual information for accurate alignment, while larger
 429 windows introduce noise that dilutes alignment signals. The framework demonstrates reasonable
 430 robustness within the 25-35 token range, validating our parameter choice and confirming consistent
 431 performance across deployment scenarios. This analysis establishes EAEV’s reliability and practical
 432 applicability under varying configuration settings. Details are provided in Appendix C.2.

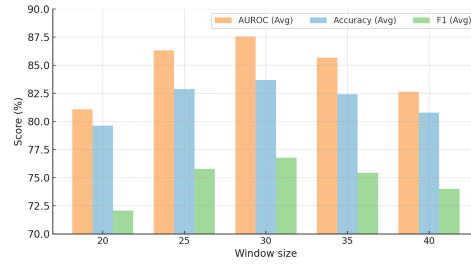
432 Table 2: Ablation study on LLaMA2-13B model. Results are reported as AUROC, Accuracy (Acc),
 433 and F1 on three benchmarks. The rightmost columns show averaged metrics across all datasets.
 434

Variant	RAGTruth			HotpotQA			DelucionQA			Average		
	AUROC	Acc	F1									
w/o Identity	85.10	82.00	74.70	86.00	81.30	73.20	84.20	81.00	75.80	85.10	81.43	74.57
w/o Semantic	83.80	81.40	73.60	85.40	81.10	73.10	83.00	80.80	75.60	84.07	81.10	74.10
w/o Consistency	85.60	82.10	74.50	83.40	79.30	71.00	81.80	78.90	73.30	83.60	80.10	72.93
w/o Stability	82.10	79.80	72.40	82.30	79.00	71.60	81.70	78.70	73.00	82.03	79.17	72.33
Full	87.89	84.29	76.85	88.12	83.53	75.59	86.65	83.22	77.92	87.55	83.68	76.79

(a) Ablation Study on Different Components



(b) Window Size Sensitivity Analysis



452 Figure 3: Ablation study results on LLaMA2-13B, showing ablation analysis on different compo-
 453 nents (left) and window size sensitivity (right).
 454

455 5 RELATED WORK

456 **Traditional Hallucination Detection** Traditional hallucination detection methods primarily leverage uncertainty estimation and self-consistency mechanisms within model outputs. Representative approaches include SelfCheckGPT, which measures semantic consistency across multiple generations (Manakul et al., 2023), and Semantic Entropy, which operates on meaning-level divergences (Farquhar et al., 2024). Recent advances explore attention-level interpretability through NoVo (Ho et al., 2025) and representational analysis of knowledge-awareness directions (Ferrando et al., 2025). While effective in controlled settings, these methods remain constrained by their reliance on internal model signals rather than explicit evidence verification.

457 **Evidence-Based Hallucination Detection in RAG** RAG environments present unique challenges 458 where hallucinations persist despite available evidence, motivating specialized detection approaches. 459 RARR employs research and revision stages for evidence attribution and consistency-based correc- 460 tion (Gao et al., 2022). FActScore provides atomic-level factual evaluation by decomposing gen- 461 erated text into verifiable claims (Min et al., 2023). CoVe introduces systematic self-verification 462 through question generation and independent answering (Dhuliawala et al., 2024). ReDeEP lever- 463 ages mechanistic interpretability to disentangle parametric and contextual knowledge contribu- 464 tions (Sun et al., 2024), while RAGTruth establishes evaluation infrastructure with fine-grained 465 annotations (Niu et al., 2024). These approaches highlight the importance of evidence-grounded 466 verification but typically operate at coarse granularities or require external verification mechanisms. 467 Our work addresses this limitation through entity-level verification within retrieved contexts, 468 providing direct evidence traceability without dependencies on external judges.

469 6 CONCLUSION

470 Hallucination detection remains critical for reliable RAG system deployment in factual applica-
 471 tions. We introduced EAEV, a novel framework that performs entity-level verification through
 472 multi-dimensional evidence alignment and counterfactual stability analysis. By distinguishing gen-
 473 uine factual support from spurious correlations, EAEV addresses fundamental challenges in RAG-
 474 based verification where hallucinated content accidentally matches retrieved text. Experimental
 475 results demonstrate substantial improvements across benchmarks and model architectures, achiev-
 476 ing 87.55% average AUROC on LLaMA2-13B. The framework’s strong generalization capabilities
 477 and practical deployability establish robust entity-level verification as a highly reliable approach for
 478 accurate hallucination detection in modern evidence-grounded generation systems.

486 ETHICS STATEMENT
487488 Our study adheres to the ICLR Code of Ethics. All experiments were conducted on publicly avail-
489 able datasets and open-source language models, as listed in Appendix A.1. No private, sensitive,
490 or personally identifiable information is involved. The primary objective of this work is to advance
491 the understanding of hallucination detection in large language models, with an emphasis on trans-
492 parency, fairness, and responsible research practices.
493494 REPRODUCIBILITY STATEMENT
495496 All models and benchmark datasets employed in this study are publicly available. Detailed descrip-
497 tions of the datasets are given in Appendix A.1.1, while the implementation details of our method
498 are provided in Appendix A.1.2. To ensure reproducibility, all experiments were conducted on four
499 NVIDIA A100 GPUs within a controlled environment, using Python 3.10.18 and PyTorch 2.2.2
500 (CUDA 11.8).
501502 REFERENCES
503

504 Amos Azaria and Tom Mitchell. The internal state of an llm knows when it's lying. In *Findings of*
505 *the Association for Computational Linguistics: EMNLP 2023*, pp. 967–976, 2023.

506 Collin Burns, Haotian Ye, Dan Klein, and Jacob Steinhardt. Discovering latent knowledge in lan-
507 guage models without supervision. In *International Conference on Learning Representations*,
508 2022.

509 Shehzaad Dhuliawala, Mojtaba Komeili, Jing Xu, Roberta Raileanu, Xian Li, Asli Celikyilmaz, and
510 Jason Weston. Chain-of-verification reduces hallucination in large language models. In *Findings*
511 *of the Association for Computational Linguistics: ACL 2024*, pp. 3563–3578, 2024.

512 Xuefeng Du, Chaowei Xiao, and Yixuan Li. Haloscope: Harnessing unlabeled
513 llm generations for hallucination detection. In *NeurIPS 2024*, 2024. URL
514 https://proceedings.neurips.cc/paper_files/paper/2024/hash/ba92705991cfbbcedc26e27e833ebbae-Abstract-Conference.html.

515 Hanyu Duan, Yi Yang, and Kar Yan Tam. Do llms know about hallucination? an empirical in-
516 vestigation of llm's hidden states. *arXiv preprint arXiv:2402.09733*, 2024. URL <https://arxiv.org/abs/2402.09733>.

517 Shahul Es, Jithin James, Luis Espinosa Anke, and Steven Schockaert. Ragas: Automated evaluation
518 of retrieval augmented generation. In *EACL 2024 (System Demonstrations)*, 2024. URL <https://aclanthology.org/2024.eacl-demo.16/>.

519 Sebastian Farquhar, Eric Hambro, Tom Rainforth, et al. Towards transparent ai: Semantic entropy
520 uncovers when language models confabulate. *Nature*, 627:767–774, 2024.

521 Javier Ferrando, Zexuan Wang, Weihao Li, Yao Zhang, Fan Yang, Lei Chen, Beichen Chen, Weize
522 Chen, Hao Zhang, Chad Steed, and Hongming Dai. Do i know this entity? knowledge awareness
523 and hallucinations in language models. In *International Conference on Learning Representations*
(ICLR), 2025.

524 Robert Friel, Masha Belyi, and Atindriyo Sanyal. Ragbench: Explainable benchmark for retrieval-
525 augmented generation systems. *arXiv preprint arXiv:2407.11005*, 2025. doi: 10.48550/arXiv.
526 2407.11005. URL <https://arxiv.org/abs/2407.11005>.

527 Yunfan Gao, Yun Xiong, Xinyu Gao, Kangxiang Jia, Jinliu Pan, Yuxi Bi, Yi Dai, Jiawei Sun, and
528 Haofen Wang. Retrieval-augmented generation for large language models: A survey. *arXiv*
529 *preprint arXiv:2312.10997*, 2023.

530 Yunxiang Gao, Zhiyong Wu, Luyang Li, Jing Wang, Xiangyu Zhang, and Gong Cheng. Rarr:
531 Researching and revising what language models say, using language models. *arXiv preprint*
532 *arXiv:2210.08726*, 2022.

540 Minsuk Ho, Jaeyoung Kim, and Kyunghyun Cho. Novo: Norm voting off hallucinations with attention
 541 heads in large language models. In *International Conference on Learning Representations (ICLR)*, 2025.

543

544 Zheng Yi Ho, Siyuan Liang, Sen Zhang, Yibing Zhan, and Dacheng Tao. Novo: Norm voting off
 545 hallucinations with attention heads in large language models. *arXiv preprint arXiv:2410.08970*,
 546 2024. URL <https://arxiv.org/abs/2410.08970>.

547

548 Xiangkun Hu, Dongyu Ru, Lin Qiu, Qipeng Guo, Tianhang Zhang, Yang Xu, Yun Luo, Pengfei
 549 Liu, Yue Zhang, and Zheng Zhang. Refchecker: Reference-based fine-grained hallucination
 550 checker and benchmark for large language models. *arXiv preprint arXiv:2405.14486*, 2024. URL
 551 <https://arxiv.org/abs/2405.14486>.

552

553 Sanjay Jain, Ziwei Sun, Yan Zhao, and Mohan Kankanhalli. Llm-check: Investigating
 554 detection of hallucinations in large language models. In *NeurIPS 2024*, 2024.
 555 URL https://proceedings.neurips.cc/paper_files/paper/2024/hash/3c1e1fdf305195cd620c118aaa9717ad-Abstract-Conference.html.

556

557 Ziwei Ji, Nayeon Lee, Rita Frieske, Tiezheng Yu, Dan Su, Yan Xu, Etsuko Ishii, Ye Jin Bang,
 558 Andrea Madotto, and Pascale Fung. Survey of hallucination in natural language generation. *ACM
 Computing Surveys*, 55(12):1–38, 2023.

559

560 Lorenz Kuhn, Yarin Gal, and Sebastian Farquhar. Semantic uncertainty: Linguistic invariances for
 561 uncertainty estimation in natural language generation. *arXiv preprint arXiv:2302.09664*, 2023.
 562 URL <https://arxiv.org/abs/2302.09664>.

563

564 Patrick Lewis, Ethan Perez, Aleksandra Piktus, Fabio Petroni, Vladimir Karpukhin, Naman Goyal,
 565 Heinrich Kütller, Mike Lewis, Wen-tau Yih, Tim Rocktäschel, et al. Retrieval-augmented
 566 generation for knowledge-intensive nlp tasks. In *Advances in Neural Information Processing Systems*,
 567 volume 33, pp. 9459–9474, 2020.

568

569 Junyi Li, Xiaoxue Cheng, Wayne Xin Zhao, Jian-Yun Nie, and Ji-Rong Wen. Halueval: A large-
 570 scale hallucination evaluation benchmark for large language models. In *Proceedings of the 2023
 Conference on Empirical Methods in Natural Language Processing*, pp. 6449–6464, 2023.

571

572 Alex Mallen, Akari Asai, Victor Zhong, Rajarshi Das, Daniel Khashabi, and Hannaneh Hajishirzi.
 573 When not to trust language models: Investigating effectiveness of parametric and non-parametric
 574 memories. In *Proceedings of the 60th Annual Meeting of the Association for Computational
 Linguistics*, pp. 9802–9822, 2022.

575

576 Potsawee Manakul, Adian Liusie, and Mark J. F. Gales. Selfcheckgpt: Zero-resource black-box
 577 hallucination detection for generative large language models. In *EMNLP 2023*, 2023. URL
 578 <https://aclanthology.org/2023.emnlp-main.557/>.

579

580 Sewon Min, Kalpesh Krishna, Xinxi Lyu, Mike Lewis, Wen-tau Yih, Pang Wei Koh, Mohit Iyyer,
 581 Luke Zettlemoyer, and Hannaneh Hajishirzi. Factscore: Fine-grained atomic evaluation of factual
 582 precision in long form text generation. In *Proceedings of the 2023 Conference on Empirical
 Methods in Natural Language Processing (EMNLP)*, pp. 12076–12100, 2023.

583

584 Cheng Niu, Yuanhao Wu, Juno Zhu, Siliang Xu, Kashun Shum, Randy Zhong, Juntong Song, and
 585 Tong Zhang. Ragtruth: A hallucination corpus for developing trustworthy retrieval-augmented
 586 language models. In *Proceedings of the 62nd Annual Meeting of the Association for Com-
 587 putational Linguistics (Volume 1: Long Papers)*, pp. 10862–10878, Bangkok, Thailand, 2024.
 588 Association for Computational Linguistics. URL <https://aclanthology.org/2024.acl-long.585>.

589

590 OpenAI. Why language models hallucinate. *arXiv preprint arXiv:2509.04664*, 2025. URL <https://arxiv.org/abs/2509.04664>.

591

592 Seongheon Park, Xuefeng Du, Min-Hsuan Yeh, Haobo Wang, and Yixuan Li. Steer llm latents for
 593 hallucination detection. *arXiv preprint arXiv:2503.01917*, 2025. URL <https://arxiv.org/abs/2503.01917>. ICML 2025 (as indicated by project materials).

594 Mobashir Sadat, Zhengyu Zhou, Lukas Lange, Jun Araki, Arsalan Gundroo, Bingqing Wang,
 595 Rakesh Menon, Md Parvez, and Zhe Feng. Delucionqa: Detecting hallucinations in domain-
 596 specific question answering. In *Findings of the Association for Computational Linguistics: EMNLP 2023*, pp. 822–835, Singapore, 2023. Association for Computational Linguistics.
 597 doi: 10.18653/v1/2023.findings-emnlp.59. URL <https://aclanthology.org/2023.findings-emnlp.59>.

600 Ben Snyder, Marius Moisescu, and Muhammad Bilal Zafar. On early detection of hallucinations in
 601 factual question answering. In *KDD 2024*, 2024. URL <https://arxiv.org/abs/2312.14183>.

603 Zhongxiang Sun, Xiaoxue Zang, Kai Zheng, Yuhang Guo, Xiaofei Xie, Lei Ma, Shouling Ji, Min
 604 Yang, Xuanyu Zhang, Lijie Hu, Yuan Yao, Lingming Zhang, Yu Pu, Lichao Sun, Qi Li, and
 605 Bo Li. Redeepl: Detecting hallucination in retrieval-augmented generation via mechanistic
 606 interpretability. *arXiv preprint arXiv:2410.11414*, 2024. URL <https://arxiv.org/abs/2410.11414>.

607 Ruizhe Tang, Xiaoman Zhang, Yifan Liu, Jing Wang, Dyi Yang, and Dragomir Radev. Medrag: A
 608 retrieval-augmented medical question answering system. *arXiv preprint arXiv:2402.13178*, 2024.

609 James Thorne, Andreas Vlachos, Christos Christodoulopoulos, and Arpit Mittal. Fever: A large-
 610 scale dataset for fact extraction and verification. In *Proceedings of EMNLP*, 2018.

611 Hugo Touvron, Louis Martin, Kevin Stone, Peter Albert, Amjad Almahairi, Yasmine Babaei, and
 612 et al. Llama 2: Open foundation and fine-tuned chat models. *arXiv preprint arXiv:2307.09288*,
 613 2023. URL <https://arxiv.org/abs/2307.09288>.

614 Yuhao Wang, Cheng Li, Cen Qu, Hao Zhao, Ruobing Zhang, Xin Liu, and Enhong Chen. Educhat:
 615 A large-scale language model-based chatbot system for intelligent education. In *Proceedings of
 616 the 62nd Annual Meeting of the Association for Computational Linguistics*, pp. 8124–8137, 2024.

617 An Yang, Baosong Yang, Beichen Zhang, Binyuan Hui, Bo Zheng, Bowen Yu, Chengyuan Li,
 618 Dayiheng Liu, Fei Huang, Haoran Wei, Huan Lin, Jian Yang, Jianhong Tu, Jianwei Zhang, Jianxin
 619 Yang, Jiaxi Yang, Jingren Zhou, Junyang Lin, Kai Dang, Keming Lu, Keqin Bao, Kexin Yang,
 620 Le Yu, Mei Li, Mingfeng Xue, Pei Zhang, Qin Zhu, Rui Men, Runji Lin, Tianhao Li, Tianyi Tang,
 621 Tingyu Xia, Xingzhang Ren, Xuancheng Ren, Yang Fan, Yang Su, Yichang Zhang, Yu Wan,
 622 Yuqiong Liu, Zeyu Cui, Zhenru Zhang, and Zihan Qiu. Qwen2.5 technical report. *arXiv preprint
 623 arXiv:2412.15115*, 2024. URL <https://arxiv.org/abs/2412.15115>.

624 Zhilin Yang, Peng Qi, Saizheng Zhang, Yoshua Bengio, William W. Cohen, Ruslan Salakhutdinov,
 625 and Christopher D. Manning. Hotpotqa: A dataset for diverse, explainable multi-hop question
 626 answering. In *Proceedings of the 2018 Conference on Empirical Methods in Natural Language
 627 Processing*, Brussels, Belgium, 2018. Association for Computational Linguistics. URL <https://aclanthology.org/D18-1259/>.

628 Xiang Yue, Boshi Wang, Kai Zhang, Ziru Jia, Yu Cheng, Huan Zhang, and Yu Su. Automatic eval-
 629 uation of attribution by large language models. In *Findings of the Association for Computational
 630 Linguistics: EMNLP 2023*, pp. 5631–5644, 2023.

631

632 A APPENDIX

633 A.1 EXPERIMENTAL DETAILS

634 A.1.1 DATASETS DETAILS

635 **RAGTruth** RAGTruth provides a controlled environment for analyzing hallucinations in standard
 636 RAG pipelines. The corpus aggregates responses from both open-source and closed-source LLMs,
 637 accompanied by meticulous word-level manual annotations and instance-level labels across three
 638 task categories: question answering, data-to-text generation, and news summarization. The dataset
 639 comprises approximately 18,000 annotated responses in total. We compute all evaluation metrics at
 640 the answer level to maintain consistency across comparisons (Niu et al., 2024).

648 **RAGBench (HotpotQA & DelucionQA)** RAGBench is a large-scale benchmark containing ap-
 649 proximately 100,000 examples with a standardized RAG schema that provides retrieved contexts and
 650 answer annotations suitable for hallucination detection tasks. The benchmark spans five domains
 651 and twelve component datasets. We utilize two representative components: (i) **HotpotQA**, a multi-
 652 hop question answering benchmark built on Wikipedia articles with sentence-level supporting facts
 653 that emphasizes cross-document reasoning capabilities; and (ii) **DelucionQA**, a domain-specific QA
 654 dataset constructed from automotive user manuals, featuring human-annotated labels that indicate
 655 whether answers contain hallucinations given the retrieved context. We adopt the benchmark’s eval-
 656 uation protocol and consistently assess performance at the answer level (Friel et al., 2025; Yang
 657 et al., 2018; Sadat et al., 2023).

658 **A.1.2 IMPLEMENTATION DETAILS**

660 We run all experiments on servers equipped with 4xNVIDIA A100 GPUs and server-grade multi-
 661 core processors. Our implementation is based on PyTorch and Hugging Face Transformers. We use
 662 LLaMA-Factory for LLM fine-tuning and inference (with LoRA). Unless otherwise specified, we
 663 employ greedy search for generation decoding, and all other parameters follow the default settings
 664 of each model.

665 For candidate construction and evidence retrieval, we retain at most 5 candidate windows per men-
 666 tion with $\text{top_bm25} = 2$ and $\text{top_embed} = 2$. Answer-side windows use $\text{window_tokens} = 30$ and
 667 $\text{stride} = 15$. For multi-dimensional alignment, we use type-adaptive weights with defaults ENT:
 668 $(0.45, 0.45, 0.10)$, NUM: $(0.25, 0.25, 0.50)$, and NP: $(0.35, 0.35, 0.30)$. We set default $\beta = 1.0$ for
 669 consistency margin. For CRS analysis, we apply four perturbation types: leave-one-out, depunc-
 670 tuating and lowercasing, compressing whitespace, and retaining only alphanumeric characters. For
 671 entity grouping, we use conservative aggregation with default $K = 2$ and $\beta_e = 1.0$. For decision
 672 rules, we scan $\tau_{\text{scm}} \in [-0.5, 0.2]$, $\tau_{\text{escm}} \in [-0.5, -0.1]$, $\tau_{\text{crs_min}} \in [0.0, 0.5]$, and $K \in \{1, 2, 3\}$ on
 673 validation sets.

674 For EAEV-guided SFT, we insert $\langle E \rangle \dots \langle /E \rangle$ markers and select $(\alpha, \gamma, w_{\min}, w_{\max})$ on validation
 675 sets. Fine-tuning uses LLaMA-Factory with LoRA, following framework defaults except for token
 676 weighting and data annotation. All hyperparameters use validation set selection, and final results
 677 report best validation configurations.

678 **A.1.3 EVALUATION METRICS**

680 Following prior works (Kuhn et al., 2023; Du et al., 2024), we employ three complementary metrics
 681 to evaluate hallucination detection performance: area under the receiver operating characteristic
 682 curve (AUROC), Accuracy, and F1 score.

684 **AUROC** measures the ability of a method to discriminate between truthful and hallucinated outputs
 685 across different decision thresholds. A higher AUROC indicates better overall ranking performance
 686 independent of a specific threshold.

687 **Accuracy** is calculated by comparing predicted labels with ground-truth annotations under a fixed
 688 threshold (e.g., 0.5 on the similarity score between the generation and the reference). It reflects the
 689 proportion of correctly classified instances but can be biased when classes are imbalanced.

690 **F1 score**, the harmonic mean of Precision and Recall, provides a balanced evaluation when both
 691 false positives and false negatives are costly. It is particularly useful in assessing detection perfor-
 692 mance under skewed class distributions.

693 Together, these metrics ensure a comprehensive assessment of both ranking quality and classification
 694 reliability in hallucination detection.

696 **A.1.4 MODEL DETAILS**

698 We conduct our experiments on three widely used large language models that represent different
 699 scales and training paradigms. **Qwen2.5-7B** (Yang et al., 2024) is an open-source model from Al-
 700 ibaba’s Qwen series, designed with improved pre-training data and instruction tuning for multilin-
 701 gual reasoning. **LLaMA2-7B** (Touvron et al., 2023) and **LLaMA2-13B** (Touvron et al., 2023) are
 part of Meta’s LLaMA2 family, which have been extensively used as backbone models in academic

702 research and industrial applications. Together, these models cover diverse capacities and training
 703 corpora, providing a representative testbed for evaluating hallucination detection methods.
 704

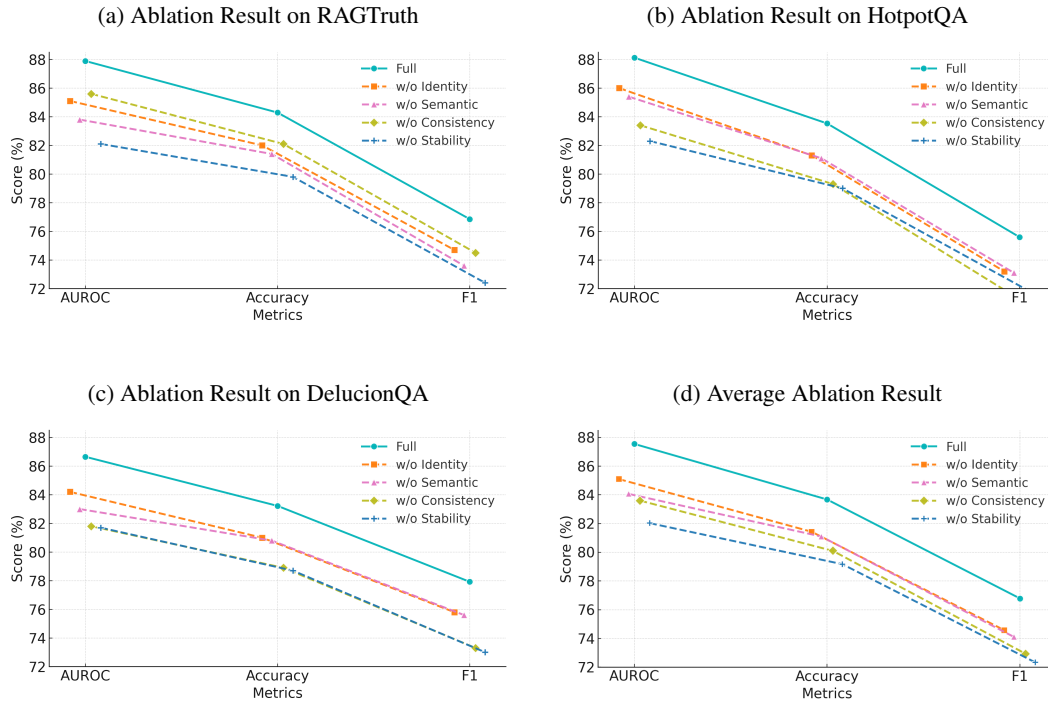
708 B DETAILS ABOUT BASELINE MODELS

712 We compare our approach against eleven representative hallucination detection baselines. Below we
 713 briefly introduce each method and its underlying intuition.
 714

- 715 • **SelfCheckGPT** (Manakul et al., 2023): A zero-resource, sampling-based detector that repeatedly
 716 queries the model to generate multiple candidate responses and then measures their consistency.
 717 Greater inconsistency across samples suggests a higher risk of hallucination, making this method effective even without external evidence.
 718
- 719 • **Semantic Entropy** (Kuhn et al., 2023): Estimates hallucination likelihood by computing linguistic
 720 invariances in token-level predictive distributions. When semantic alternatives diverge
 721 strongly in probability space, the model exhibits higher semantic entropy, indicating uncertainty and potential unreliability in factual grounding.
 722
- 723 • **LLM-Check** (Jain et al., 2024): Probes internal hidden states of LLMs with lightweight classifiers to directly flag hallucinations. By exploiting activation-level features, LLM-Check can
 724 detect subtle factual errors that do not manifest at the surface level but are encoded within the
 725 model’s latent representations.
 726
- 727 • **Linear Probe** (Duan et al., 2024): A straightforward but effective baseline that trains linear
 728 classifiers on the hidden states of LLMs. By mapping internal activations to truthfulness labels, Linear Probe directly tests how much factuality information is encoded within raw model
 729 representations.
 730
- 731 • **HaloScope** (Du et al., 2024): Leverages large quantities of unlabeled LLM outputs and applies
 732 energy-based and representation-driven detectors. By clustering semantic patterns across generations,
 733 HaloScope effectively identifies outliers that correspond to hallucinated claims with minimal supervision.
 734
- 735 • **EarlyDetect** (Snyder et al., 2024): A proactive detector that monitors generation in-progress.
 736 By analyzing partial outputs and their factual signals, EarlyDetect aims to catch hallucinations
 737 early, before the model produces fully misleading answers, thus enabling faster correction or
 738 intervention.
 739
- 740 • **NoVo** (Ho et al., 2024): Stands for Norm Voting off hallucinations. This method measures the
 741 norms of attention heads and aggregates their “votes” to infer factual reliability. It leverages
 742 attention-level interpretability to highlight internal disagreement patterns that often precede
 743 hallucinated generations.
 744
- 745 • **RAGAS** (Es et al., 2024): Focuses on retrieval-augmented settings by breaking down model
 746 outputs into atomic statements and verifying each against retrieved passages. Faithfulness is
 747 quantified as the ratio of supported claims, allowing fine-grained detection of unsupported or
 748 fabricated content.
 749
- 750 • **RefChecker** (Hu et al., 2024): Constructs structured knowledge graphs from model outputs
 751 and checks their alignment with external references. This graph-based perspective enables
 752 detection of hallucinations that may not be obvious at sentence level but become evident when
 753 relational consistency is examined.
 754
- 755 • **ReDEeP** (Sun et al., 2024): Employs mechanistic interpretability in retrieval-augmented generation (RAG). By tracing attention flow from queries to evidence passages, ReDEeP identifies whether the model’s factual claims are truly supported by retrieved documents or merely spurious correlations.
 756
- 757 • **TSV** (Park et al., 2025): Introduces the Truthfulness Separator Vector, which perturbs latent
 758 representations during inference to evaluate the stability of factual claims. Robust claims remain
 759 separable under perturbations, while hallucinated ones collapse, offering a novel perspective on truthfulness detection.
 760

756 Table 3: Ablation study on LLaMA2-13B model. Results are reported as AUROC, Accuracy (Acc),
 757 and F1 on three benchmarks. The rightmost columns show averaged metrics across all datasets.
 758

Variant	RAGTruth			HotpotQA			DelucionQA			Average		
	AUROC	Acc	F1									
w/o Identity	85.10	82.00	74.70	86.00	81.30	73.20	84.20	81.00	75.80	85.10	81.43	74.57
w/o Semantic	83.80	81.40	73.60	85.40	81.10	73.10	83.00	80.80	75.60	84.07	81.10	74.10
w/o Consistency	85.60	82.10	74.50	83.40	79.30	71.00	81.80	78.90	73.30	83.60	80.10	72.93
w/o Stability	82.10	79.80	72.40	82.30	79.00	71.60	81.70	78.70	73.00	82.03	79.17	72.33
Full	87.89	84.29	76.85	88.12	83.53	75.59	86.65	83.22	77.92	87.55	83.68	76.79



789 Figure 4: Detailed ablation results on LLaMA2-13B. Results are shown on RAGTruth (top-left),
 790 HotpotQA (top-right), DelucionQA (bottom-left), and averaged across datasets (bottom-right).
 791

793 C ADDITIONAL RESULTS

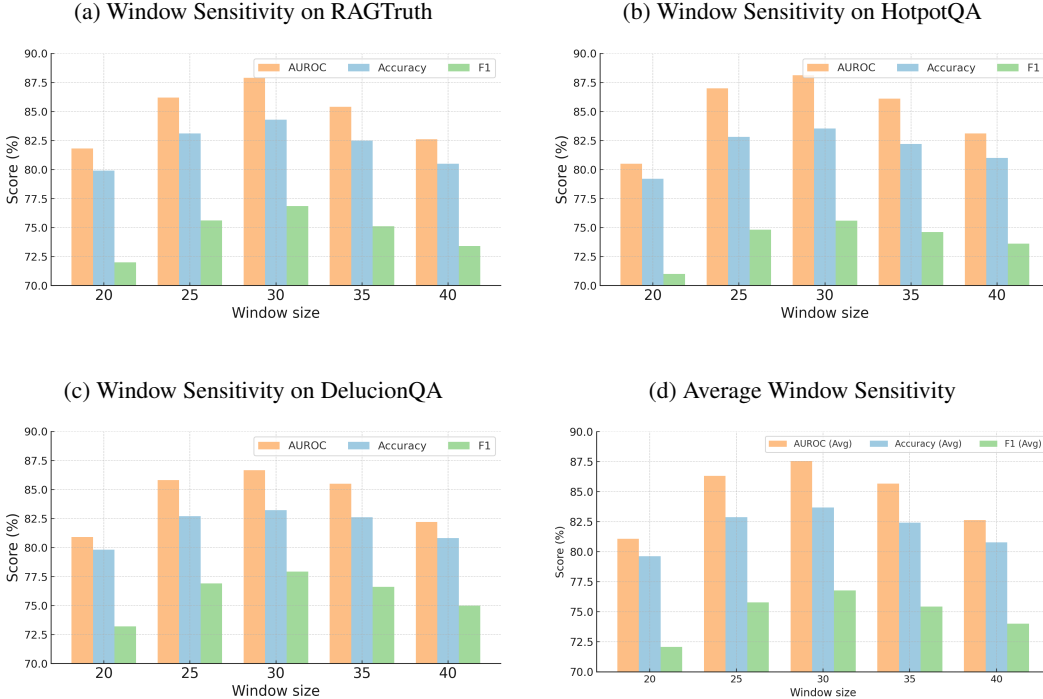
795 C.1 COMPLETE ABLATION STUDY

797 We provide comprehensive ablation analysis across all datasets and model architectures to validate
 798 each component’s contribution. Table 3 presents the complete ablation results on LLaMA2-
 799 13B, while Figures 4a through 4d show detailed performance degradation patterns across individual
 800 datasets and averaged results.

801 The ablation visualizations reveal distinct component contributions across different evaluation sce-
 802 narios. Counterfactual stability analysis demonstrates the most substantial impact across all datasets,
 803 with removal leading to 5.52 AUROC points average degradation. This consistent pattern con-
 804 firms the necessity of distinguishing genuine evidence support from spurious correlations regardless
 805 of dataset characteristics. Consistency alignment shows particularly pronounced effects on Hot-
 806 potQA and DelucionQA, where quantitative verification becomes critical for multi-hop reasoning
 807 and domain-specific content. Semantic alignment exhibits stronger influence on RAGTruth, reflect-
 808 ing its importance for handling paraphrased expressions in general knowledge contexts. Identity
 809 alignment provides steady baseline performance through exact matching across all evaluation set-
 810 tings.

810
 811 Table 4: Sensitivity to answer-side window length (LLaMA2-13B). Results are reported as AUROC,
 812 Accuracy (Acc), and F1 on three benchmarks. The rightmost columns show averaged metrics across
 813 all datasets.

814 815 window size	816 RAGTruth			817 HotpotQA			818 DelucionQA			819 AUROC		
	820 AUROC	821 Acc	822 F1	823 AUROC	824 Acc	825 F1	826 AUROC	827 Acc	828 F1	829 AUROC	830 Avg Acc	831 Avg F1
20	81.81	79.95	72.04	80.52	79.27	71.03	80.90	79.85	73.28	81.07	79.63	72.07
25	86.23	83.17	75.64	87.03	82.81	74.82	85.81	82.70	76.96	86.33	82.87	75.77
30	87.89	84.29	76.85	88.12	83.53	75.59	86.65	83.22	77.92	87.55	83.68	76.79
35	85.42	82.51	75.15	86.13	82.26	74.64	85.53	82.68	76.60	85.67	82.43	75.43
40	82.65	80.53	73.42	83.16	81.04	73.68	82.27	80.83	75.01	82.63	80.77	74.00



844 Figure 5: Parameter sensitivity analysis of EAEV under different answer-side window lengths.
 845 Results are shown on RAGTruth (top-left), HotpotQA (top-right), DelucionQA (bottom-left), and
 846 averaged across datasets (bottom-right).

848 The balanced degradation curves across datasets validate our multi-dimensional design philosophy.
 849 Each alignment dimension addresses distinct verification challenges while maintaining complemen-
 850 tary effects, with no single component dominating performance. The stability analysis com-
 851 ponent’s consistent importance across all scenarios confirms the practical value of robustness testing
 852 in evidence-based verification systems.

C.2 SENSITIVITY ANALYSIS

856 Parameter sensitivity analysis demonstrates EAEV’s robustness across different configuration set-
 857 tings. Table 4 provides detailed performance under varying answer-side window lengths, while
 858 Figures 5a through 5d illustrate the characteristic inverted-U performance curves across individual
 859 datasets.

860 The sensitivity visualizations reveal consistent optimal performance at 30-token windows across all
 861 datasets, with graceful degradation patterns for both smaller and larger window sizes. RAGTruth
 862 shows the sharpest sensitivity curve, indicating that fine-grained annotations benefit most from
 863 optimal contextualization. HotpotQA exhibits broader stability around the optimum, reflecting the
 864 method’s robustness for multi-hop reasoning tasks. DelucionQA demonstrates intermediate sensi-

864
 865 **Task.** Given a question, supporting passages, and a model answer, mark any unsupported or contradic-
 866 tory entity mentions in the answer using `<E>...</E>` tags. Keep the original answer text and only
 867 add tags.
 868 **Question.** `{String}`
 869 **Supporting Passages:**
 870 `<W1> {String} </W1>`
 871 `<W2> {String} </W2>`
 872 `<W3> {String} </W3>`
 873 **Original Answer.** `{String}`
 874 **Instructions.**
 875 • Mark entities contradicted by the supporting passages.
 876 • Mark entities lacking sufficient evidence support.
 877 • Preserve all original text—only add `<E>...</E>` tags.
 878 • Focus on named entities, dates, numbers, and key factual claims.
 879
 880 **Expected Output.** *Answer text with `<E>...</E>` tags around unsupported entities.*

882
 883 Figure 6: Prompt template for EAEV-guided supervised fine-tuning.
 884

885 tivity patterns, suggesting balanced requirements between contextual information and noise control
 886 in domain-specific settings.
 887

888 Performance degradation below 25 tokens reflects insufficient contextual information for accurate
 889 alignment assessment, while degradation above 35 tokens indicates noise introduction from irrele-
 890 vant content. The framework maintains reasonable stability within the 25-35 token range across all
 891 datasets, supporting practical deployment flexibility. These results validate our parameter selection
 892 methodology and confirm EAEV’s reliability under varying configuration requirements.

893 D DETAILS FOR PROMPT TEMPLATE

896 The EAEV-guided supervised fine-tuning transforms entity verification into an executable annota-
 897 tion generation task. We design a structured prompt that enables models to learn EAEV’s multi-
 898 dimensional alignment patterns through standard supervised training while maintaining evidence
 899 traceability.

900 The prompt design follows several key principles to ensure effective knowledge transfer from
 901 EAEV’s verification framework. The task description explicitly requires minimal modification
 902 where only annotation tags are added without altering original answer text. Supporting passages
 903 are clearly delineated with window markers (`<W1>`, `<W2>`, `<W3>`) to maintain precise evidence
 904 traceability throughout verification. The instructions distinguish between contradicted entities and
 905 those lacking sufficient support, reflecting EAEV’s multi-dimensional alignment assessment.

906 This structured approach enables standard supervised fine-tuning to learn sophisticated verification
 907 patterns while preserving interpretability through direct evidence grounding. The prompt trans-
 908 forms entity-level hallucination detection into a sequence labeling task that models can learn through
 909 token-weighted cross-entropy loss, directly implementing the supervision mechanism described in
 910 Section 3.

911 E USAGE CLAIM OF LLMs

914 We use LLM for grammar and spelling checks only, with prompt “Proofread the sentences”. All
 915 conceptual development, analysis, writing, and editing were carried out solely by the authors without
 916 LLM assistance.

917